Phonon-assisted excitation energy transfer in photosynthetic systems*

Hao Chen(陈浩), Xin Wang(王信), Ai-Ping Fang(方爱平)†, and Hong-Rong Li(李宏荣)‡

Department of Applied Physics, Xi'an Jiaotong University, Xi'an 710049, *China*

(Received 2 February 2016; revised manuscript received 20 May 2016; published online 2 August 2016)

The phonon-assisted process of energy transfer aiming at exploring the newly emerging frontier between biology and physics is an issue of central interest. This article shows the important role of the intramolecular vibrational modes for excitation energy transfer in the photosynthetic systems. Based on a dimer system consisting of a donor and an acceptor modeled by two two-level systems, in which one of them is coupled to a high-energy vibrational mode, we derive an effective Hamiltonian describing the vibration-assisted coherent energy transfer process in the polaron frame. The effective Hamiltonian reveals in the case that the vibrational mode dynamically matches the energy detuning between the donor and the acceptor, the original detuned energy transfer becomes resonant energy transfer. In addition, the population dynamics and coherence dynamics of the dimer system with and without vibration-assistance are investigated numerically. It is found that, the energy transfer efficiency and the transfer time depend heavily on the interaction strength of the donor and the high-energy vibrational mode, as well as the vibrational frequency. The numerical results also indicate that the initial state and dissipation rate of the vibrational mode have little influence on the dynamics of the dimer system. Results obtained in this article are not only helpful to understand the natural photosynthesis, but also offer an optimal design principle for artificial photosynthesis.

Keywords: excitation energy transfer, high-energy intramolecular vibrational motion, resonant coherent transfer

PACS: 82.20.Rp, 42.50.Nn, 42.50.Wk **DOI:** 10.1088/1674-1056/25/9/098201

1. Introduction

To date, plenty of progress in experimental, theoretical, and computational research on the mechanism of efficient excitation energy transfer (EET) in a photosynthesis system have been done.[1–7] Some mechanisms have been proposed to explain the unusual coherent nature of excitation transport, thus showing us some insights into the potential functional role of such quantum features. Now, it is known that the functionality of a natural multichromophoric complex depends mainly on the strength and structure of interactions among electronic states and is dramatically affected by the vibrational degrees of freedom associated either to the complex itself or to its environment.[8–12] By interacting with the electronic states, the phonon environment influences electronic excitation dynamics in various ways depending on the vibrational frequency and the coupling strength.[5] Firstly, phonon modes arising from the low-energy protein vibrations and the solvent have a continuous distribution of frequencies that are below or comparable to the thermal energy scale, $k_{\mathrm{B}}T$, and couple to the electronic states weakly comparing with the coupling strength among electronic states. By inducing thermal fluctuations of on-site energies, these modes perturb the system enough to suppress destructive interference and broaden its spectral lines,[5,13–16] thus leading to an enhanced excitation transfer between energetically close excitation states. Secondly, phonon modes with high energy and well-localized frequencies are revealed, by spectroscopy studies,[17–24] the active participation during the excitation dynamics. These modes originate from intramolecular vibrations and couple to the electronic states with strength comparable to that of inter-site electronic interaction.[25–28] The quantum mechanical features of the high-energy vibrational modes are significant even at ambient temperatures[8] and their influence in energy transport in a variety of natural molecular systems is currently of central interest.[23,24,29–31]

In this work, we focus on the important role of the high-energy vibrational modes for electronic excitation transport in a situation similar to that in cryptophyte antennae protein phycoerythrin 545 (PE545).[27,32] In PE545, site energy differences $|\varepsilon_m - \varepsilon_n|$ are very large in comparison to inter-site electronic interaction V_{mn}, which is comparable to the couplings between high-energy vibrational modes and electronic states. In this situation, excitation energy is highly localized to a particular site and hardly transports to the next site without external influences. For instance, the largest coupling of inter-site electronic interactions in PE545 is $V = 92$ cm^{-1} between the central pigments $\mathrm{PEB}_{50\mathrm{C}}$ and $\mathrm{PEB}_{50\mathrm{D}}$, while their energy difference is about 1040 cm^{-1}.[28] The localized vibrational mode at $\omega = 1111$ cm^{-1} is in close resonance with

*Project supported by the National Natural Science Foundation of China (Grant No. 11174233).

†Corresponding author. E-mail: apfang@mail.xjtu.edu.cn

‡Corresponding author. E-mail: hrli@mail.xjtu.edu.cn

© 2016 Chinese Physical Society and IOP Publishing Ltd

the transition between PEB_{50C} and PEB_{50D}. The coupling between the mode and the electronic states of the two sites is $g = 267\ \mathrm{cm}^{-1}$ ($g = \omega\sqrt{s} = 1111\ \mathrm{cm}^{-1} \times \sqrt{0.0578} \approx 267\ \mathrm{cm}^{-1}$, where ω is the frequency of the intramolecular vibrational mode and s is the Huang–Rhys factor),[28] which is comparable to $V = 92\ \mathrm{cm}^{-1}$. We will investigate the fundamental mechanism of a bridge-like role of quasi-resonant vibrations for the excitonic transitions in the above situation by considering a typical dimer model, which has also been mentioned by Avinash Kolli previously.[28] We reveal, by numerical calculation, the optimal parameters in high-energy-phonon-assisted EET in the large-detuning condition.

In our model, which is based on the PEB_{50C} and PEB_{50D} system, the strength of coupling between a high-energy vibrational mode and the donor's electronic state is comparable to that of the dipole–dipole interaction between the donor and the acceptor, while the phonon bath of the environment couples to the donor and the acceptor weakly. Hence a polaron-presentation is needed to describe the electronic excitation dynamics under the influence of the high-energy vibrational modes.[33,34] In the polaron frame, we derived an effective Hamiltonian revealing the coherent energy transition among the donor, the acceptor and the high-energy vibrational mode. We present and discuss the numerical results to quantify the impact of the high-energy vibrational mode upon the dynamics and efficiency of EET in the system.

This paper is organized as follows. In Section 2, we derive an effective Hamiltonian within the polaron frame and show the basic mechanism of detuned high-energy-phonon-assisted energy transfer by analyzing the effective Hamiltonian. In Section 3, we numerically calculated the population dynamics and coherence dynamics of the system to reveal the detailed influence of the high-energy vibrational mode on the transfer efficiency and transfer time. The conclusion is made in Section 4.

2. Analysis

In this section, we consider a dimer system consisting of a donor and an acceptor described by two two-level systems,[5] in which the donor is coupled to a quantized vibrational mode describing the high-energy intramolecular vibration. To simplify the expression we set $\hbar = 1$, then the dimer and the vibrational mode are described by the bare Hamiltonian $H_{\mathrm{e}} = \varepsilon_1\sigma_1^+\sigma_1^- + \varepsilon_2\sigma_2^+\sigma_2^-$ and $H_v = \omega b^\dagger b$, respectively. The donor and the acceptor are coupled by a dipole–dipole interaction with the form $H_{\mathrm{e-e}} = V_{12}\left(\sigma_1^+\sigma_2^- + \sigma_2^+\sigma_1^-\right)$. The Hamiltonian describing the linear interaction between the donor and the quantized vibrational mode reads[28] $H_{\mathrm{e-v}} = g(b^\dagger + b)\sigma_1^+\sigma_1^-$. In the above, $\sigma_1^+ = |e_1\rangle\langle g_1|$ ($\sigma_2^+ = |e_2\rangle\langle g_2|$) corresponds to the creation operator of an excitation on the donor (acceptor) with energy ε_1 (ε_2), and V_{12} denotes the electronic coupling between the donor and the acceptor. $b^\dagger$ (b) corresponds to the creation (annihilation) operator of the vibrational mode with frequency ω, and g represents the coupling of the donor to the vibrational mode.

Then the Hamiltonian describing the combined system is

$$H = \varepsilon_1\sigma_1^+\sigma_1^- + \varepsilon_2\sigma_2^+\sigma_2^- + \omega b^\dagger b + V_{12}\left(\sigma_1^+\sigma_2^- + \sigma_2^+\sigma_1^-\right) + g(b^\dagger + b)\sigma_1^+\sigma_1^-. \quad (1)$$

In the above Hamiltonian, the energy scale of the vibrational mode, electronic coupling and exciton–phonon coupling are comparable, so the influence of the vibrational mode cannot be treated as a perturbation to the electronic states. We need to move into a polaron frame where electronic couplings are renormalized and fluctuate due to the interaction with the vibrational modes. Under certain conditions, the electronic coupling fluctuations can be treated as a perturbation, and a second-order master equation can be derived in a standard way to capture non-Markovian and non-equilibrium effects of the vibrational mode in the intermediate regime.[34] To understand how exactly the vibrational mode influences the electronic coupling, we need to derive the Hamiltonian of the combined system in the interaction picture. Before doing this, we perform a polaron transformation of the exciton–phonon Hamiltonian prior to a perturbative expansion with respect to a redefined system-vibration interaction in the transformed frame. The weakly coupled phonon bath of the environment is not considered temporarily because it does not affect the fundamental mechanism showing in this section. It will be included in part of the numerical study to capture the indirect influence of a phonon bath on EET through the high-energy vibrational mode.

We begin our analysis by moving into the polaron frame[33,34] defined by the transformation $\widetilde{H} = \mathrm{e}^{S}H\mathrm{e}^{-S}$, where $S = \sigma_1^+\sigma_1^-(gb^\dagger/\omega - g^*b/\omega)$. Within this transformed frame, the Hamiltonian within the single-excitation subspace[5] becomes

$$\widetilde{H} = \widetilde{\varepsilon}_1\sigma_1^+\sigma_1^- + \widetilde{\varepsilon}_2\sigma_2^+\sigma_2^- + \omega b^\dagger b + V_{12}\left(B_{12}\sigma_1^+\sigma_2^- + B_{12}^\dagger\sigma_2^+\sigma_1^-\right), \quad (2)$$

where the energy of the donor is now shifted by its corresponding reorganisation energy caused by interaction with the vibrational mode, such that $\widetilde{\varepsilon}_1 = \varepsilon_1 - |g|^2/\omega$, while energy of the acceptor is unchanged, $\widetilde{\varepsilon}_2 = \varepsilon_2$, and $B_{12} = \mathrm{e}^{g\left(b^\dagger - b\right)/\omega}$.

We now separate $\widetilde{H}$ into two parts, a non-interacting Hamiltonian $\widetilde{H}_0 = \widetilde{\varepsilon}_1\sigma_1^+\sigma_1^- + \widetilde{\varepsilon}_2\sigma_2^+\sigma_2^- + \omega b^\dagger b$ and an interaction Hamiltonian

$$\widetilde{H}_1 = V_{12}\left(\mathrm{e}^{g\left(b^\dagger - b\right)/\omega}\sigma_1^+\sigma_2^- + \mathrm{e}^{g\left(b - b^\dagger\right)/\omega}\sigma_2^+\sigma_1^-\right).$$

Now we move into the interaction picture by the transformation $\widetilde{H}_{\mathrm{I}} = \mathrm{e}^{-\mathrm{i}\widetilde{H}_0 t/\hbar}\widetilde{H}_1\,\mathrm{e}^{\mathrm{i}\widetilde{H}_0 t/\hbar}$, and obtain

$$\widetilde{H}_{\mathrm{I}} = V_{12}\frac{g}{\omega}\left(\mathrm{e}^{-\mathrm{i}(\omega+\Delta)t/\hbar}b^\dagger\sigma_1^+\sigma_2^- - \mathrm{e}^{\mathrm{i}(\omega-\Delta)t/\hbar}b\sigma_1^+\sigma_2^-\right.$$

$$+ e^{i(\omega+\Delta)t/\hbar} b\sigma_2^+\sigma_1^- - e^{-i(\omega-\Delta)t/\hbar} b^\dagger\sigma_2^+\sigma_1^-\big), \quad (3)$$

where $\Delta = \widetilde{\varepsilon}_1 - \widetilde{\varepsilon}_2$.

From the above interaction Hamiltonian $\widetilde{H}_{\rm I}$, we can see that if the frequency of the vibrational mode resonates to the detuning between the donor and the acceptor, i.e., $\omega = \Delta$, the first and the third term of $\widetilde{H}_{\rm I}$ oscillate quickly and can be neglected, the effective Hamiltonian is then

$$\widetilde{H}_{\rm I_{eff}} = g_{\rm eff}\left(b\sigma_1^+\sigma_2^- + b^\dagger\sigma_2^+\sigma_1^-\right), \quad (4)$$

where $g_{\rm eff} = -V_{12}g/\omega$ is the effective coupling strength.

The above effective interaction Hamiltonian $\widetilde{H}_{\rm I_{eff}}$ indicates a coherent energy transfer among the donor, the acceptor and the vibrational mode. The term $b^\dagger\sigma_2^+\sigma_1^-$ shows, in condition that the vibrational mode is in close resonance with the excitonic transition, the donor transfers from its exited state $|e_1,n\rangle$ to its ground state $|g_1,n+1\rangle$ by emitting one photon that is resonant to the transition between $|g_2\rangle$ and $|e_2\rangle$, with one phonon being created in the vibrational mode. Then the acceptor is excited and the EET process turns out to be efficient because it satisfies energy conservation. This process is illustrated in Fig. 1.

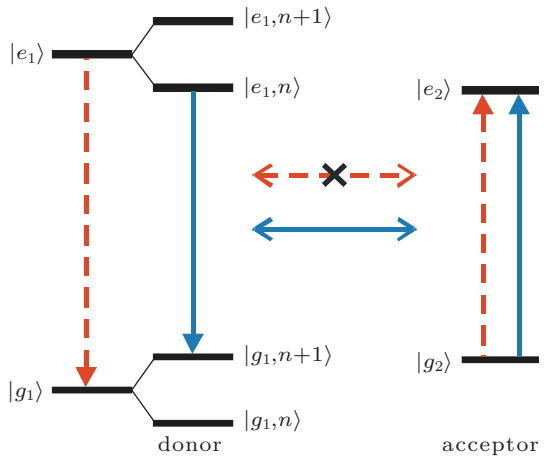


Fig. 1. (color online) Configurations of the energy levels and transitions. The red (dashed) arrow lines represent the original detuned energy transfer process which hardly succeed due to the mismatched energy levels. The blue (solid) arrow lines show the phonon-assisted energy transfer process.

3. Numerical results

In the above section, we have revealed that the physical foundation of the efficient energy transfer in the largely detuned dimer system is a coherent energy exchange among the donor, the acceptor and the high-energy vibrational mode, which is described by the effective Hamiltonian in polaron frame (Eq. (4)). To quantify the impact of the high-energy vibrational mode upon the dynamics and efficiency of EET in the dimer system, we will present and discuss the numerical results in this section. To include the influence of the weakly coupled environment, we will use the master equation in Lindblad form to calculate the combined system's evolution. Since the effective Hamiltonian is derived in the condition that $\omega = \Delta$, we use the original Hamiltonian H in Eq. (1) to do numerical calculation. The original Hamiltonian H contains the coherent energy exchange not only when $\omega = \Delta$, but also when ω is close to Δ. So we use H to numerically study the parameter-dependence of the EET without deviating from the key mechanism.

In our calculation, we do not take the light-absorption process into account, but start from the state that the donor has been excited and the acceptor is in ground state. The vibrational mode is assumed in a thermal equilibrium state like

$$\mu(0) = \sum_n \frac{n_{\rm th}^n}{(n_{\rm th}+1)^{n+1}} |n\rangle\langle n|,$$

since $\mu(0)$ is only an incoherent mixed state with different Fock states, thus a Fock state presentation is good enough to capture the main influence of the vibrational mode on EET and is of simplicity in calculation. Then we consider the energy transfer from the initial state

$$\rho(0) = |e_1\rangle\langle e_1| \otimes |g_2\rangle\langle g_2| \otimes |n\rangle\langle n|. \quad (5)$$

Energy in the donor will transfer to the acceptor with the help of a phonon with time evolving. Irreversible energy dissipation occurs because of the coupling to the environment and the sink pigments. So two kinds of energy dissipation are taken into account in the calculation. The first part is that from the donor, the acceptor and the high-energy vibrational mode to the heat bath of the environment; while the second part is from the acceptor to the sink pigments. We define the energy dissipated in the second part as effectively transferred energy.

The master equation to describe the whole energy transfer procedure has the following form:

$$\frac{d\hat{\rho}}{dt} = -i[H,\hat{\rho}] + L_{\rm diss}(\hat{\rho}), \quad (6)$$

where the dissipation is considered as a Lindblad term

$$\begin{aligned} L_{\rm diss}(\hat{\rho}) = & \sum_{i=1,2} \kappa_i \left(\sigma_-^i\hat{\rho}\sigma_+^i - \frac{1}{2}\{\sigma_+^i\sigma_-^i,\hat{\rho}\}\right) \\ & + \gamma(n_{\rm th}+1)\left(b\hat{\rho}b^\dagger - \frac{1}{2}\{b^\dagger b,\hat{\rho}\}\right) \\ & + \gamma n_{\rm th}\left(b^\dagger\hat{\rho}b - \frac{1}{2}\{bb^\dagger,\hat{\rho}\}\right), \end{aligned} \quad (7)$$

where $\{\hat{A},\hat{B}\}$ denotes the anticommutator of operator $\hat{A}$ and operator $\hat{B}$ ($\{\hat{A},\hat{B}\} = \hat{A}\hat{B} + \hat{B}\hat{A}$). Here, $\kappa_2 = \kappa_{2_0} + \kappa_{2_e}$, where κ_{2_0} is the environmental dissipation rate and κ_{2_e} is the sink rate which represents the effective energy transfer.

In last section, we have derived an effective interaction Hamiltonian $\widetilde{H}_{\rm I_{eff}}$ to reveal the coherent energy transfer process among the donor, the acceptor and the vibrational mode, now we study the population dynamics of the system by solving the above master equation numerically. We define $P_{\rm D} =$

$\langle\sigma_+^1\sigma_-^1\rangle = \mathrm{Tr}\left(\sigma_+^1\sigma_-^1\rho\right)$ and $P_\mathrm{A} = \langle\sigma_+^2\sigma_-^2\rangle = \mathrm{Tr}\left(\sigma_+^2\sigma_-^2\rho\right)$ as the probabilities of the donor and the acceptor being in their excited state, respectively. The mean number of the phonon is $N = \langle b^\dagger b\rangle = \mathrm{Tr}\left(b^\dagger b\rho\right)$. We show the population dynamics with and without the coupling between the donor and the vibrational mode in Figs. 2(a) and 2(b). The calculation parameters are chosen comparing with the coupling strength V_{12},

$$\frac{\varepsilon_1-\varepsilon_2}{V_{12}} = 10, \quad \frac{\omega}{V_{12}} = 10, \quad \frac{g}{V_{12}} = 1.5,$$
$$\frac{\kappa_1}{V_{12}} = \frac{\kappa_{2_0}}{V_{12}} = 0.0005, \quad \frac{\kappa_{2_e}}{V_{12}} = 0.15, \quad \frac{\gamma}{V_{12}} = 0.05, \quad (8)$$

which matches the ratios of those parameters in the real PE545 system. Here, V_{12}^{-1} is used as the unit of evolution time in this paper.

From Fig. 2(a), we find that the acceptor can hardly be excited when the coupling between the donor and the vibrational mode vanishes. This matches the known case that energy transfer between two two-level systems with large detuning can hardly occur. On the contrary, figure 2(b) shows the coherent energy transfer process among the donor, the acceptor and the vibrational mode. When P_A goes down from 1 to 0, the probability of the acceptor being excited increases with increasing the mean number of the phonon as well. The oscillation of P_A and N is caused by the energy exchange between the donor and the acceptor. This dynamics matches the process described by the effective Hamiltonian $b^\dagger\sigma_2^+\sigma_1^-$. Then from the population dynamics, we find that the interaction to the vibrational mode converts the original detuned EET process to a coherent resonant EET process, thus making the energy transfer from the donor to the acceptor much easier.

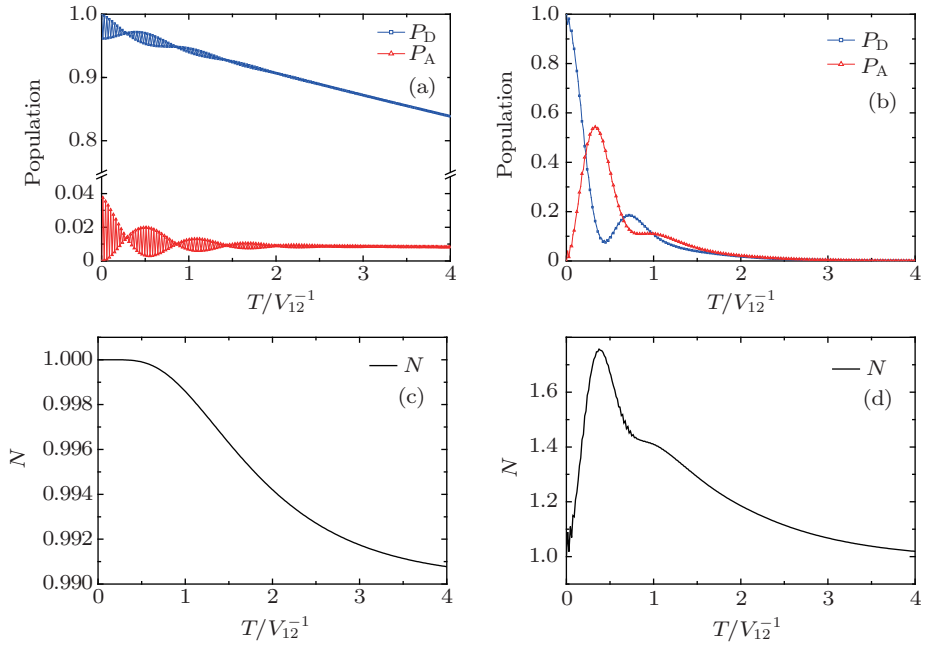


Fig. 2. (color online) Numerical results for population dynamics of the donor (blue solid line with open squares), the acceptor (red solid line with open up triangles) and the vibrational mode (black solid line), the coupling between the donor and the vibrational mode is $g/V_{12} = 0$ in panels (a) and (c), while that in panels (b) and (d) is $g/V_{12} = 1.5$. Other parameters used here are the same as those in Eq. (8).

In our model, the energy transfer efficiency (η) and average transfer time (τ), respectively, are defined by integrals[14,35–37]

$$\eta = \int_{t_0}^{t} 2\kappa_{2_\mathrm{e}}\rho_{\mathrm{ee}}^{(2)}\left(t'\right)\mathrm{d}t', \quad (9)$$

$$\tau = \eta^{-1}\int_{t_0}^{t} 2\kappa_{2_\mathrm{e}}t'\rho_{\mathrm{ee}}^{(2)}\left(t'\right)\mathrm{d}t', \quad (10)$$

where $\rho_{\mathrm{ee}}^{(2)}$ is the probability that the acceptor is in the excited state. The energy transfer efficiency refers to the total probability that the excitation is transferred to the sink pigment, where the energy is used to stimulate charge separation. From the above numerical results we know that with the help of the vibrational mode, the excitation is easier to be transferred to the acceptor and then be used in charge separation. We know from the theoretical analysis that the effective coupling strength $g_\mathrm{eff} = -V_{12}g/\omega$ is proportional to g. Then with a larger g, the process described by $g_\mathrm{eff}\left(b\sigma_1^+\sigma_2^- + b^\dagger\sigma_2^+\sigma_1^-\right)$ becomes more important among all processes during EET. So the energy transfer efficiency must be higher when the coupling between donor and vibrational mode exists. The relationship between efficiency and the coupling strength is shown in Fig. 3(a). We find that the efficiency is less than 20% without the help of the vibrational mode ($g/V_{12} = 0$). But with the increasing of the coupling strength g, the efficiency η increases rapidly until g/V_{12} goes to about 1. Then the efficiency nearly reaches to its saturation value under the limitation of some other factors.

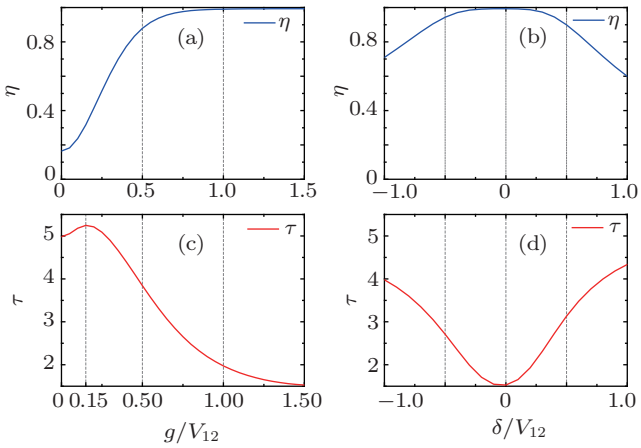


Fig. 3. (color online) Numerical results for (a) efficiency variation $\eta(g)$, (b) efficiency variation $\eta(\delta)$, (c) transfer time variation $\tau(g)$, and (d) transfer time variation $\tau(\delta)$. Other parameters used here are the same as those in Eq. (8).

It is not enough for photosynthetic organisms to transfer the energy with a high efficiency, the transfer process should also be within a short time scale. To show the influence of the vibrational mode on transfer time, we graph the average transfer time as a function of the coupling strength in Fig. 3(c). It can be seen that the longest transfer time occurs when g/V_{12} is about 0.15, with increasing of g, the transfer time decreases until it reaches to its saturated state. That is to say, the vibrational mode is helpful to enhance the transfer efficiency and make shorter the average transfer time. A larger coupling strength offers more efficiency and shorter transfer time.

The above numerical results are achieved in the situation that the vibration is resonant to the detuning between the donor and the acceptor, that is to say $\delta = \omega - (\varepsilon_1 - \varepsilon_2) = 0$. To take the non-resonant situation account, we illustrate $\eta(\delta)$ and $\tau(\delta)$ in Figs. 3(b) and 3(d), respectively. As is illustrated, the efficiency of EET decreases quickly while the transfer time increases with the increasing of $|\delta|$.

In addition, we have also investigated the dependence of transfer efficiency and transfer time on the phonon number n of the initial state of the vibrational mode (not shown here). We found that the initial state only affects the dynamics of the dimer system slightly. We conclude that a higher environmental temperature does not contribute more to energy transfer than a low temperature by the present high-energy-phonon-assisted mechanism. This is opposite to that of a low-energy-phonon-assisted mechanism.[38] Besides, the dissipation rate γ associated to the high-energy vibrational mode also affects the transfer efficiency and the transfer time in a neglectful extent.

The parameter-dependence of the EET shows that the high-energy vibrational mode plays a significant role in enhancing EET. It can be seen, from the effective Hamiltonian $b^\dagger\sigma_2^+\sigma_1^-$, that the coherent energy transfer among the donor, the acceptor and the vibrational mode is the key process in effective EET. Then, in order to investigate whether or not the coupling to the vibrational mode can influence the coherence of EET, $\langle\sigma_2^+\sigma_1^-\rangle$ was calculated and illustrated in Fig. 4(a). When the coupling exists, the coherence reaches to its minimum value just at the time when the phonon-assisted energy transfer occurs. This feature does not appear in the non-coupling situation.

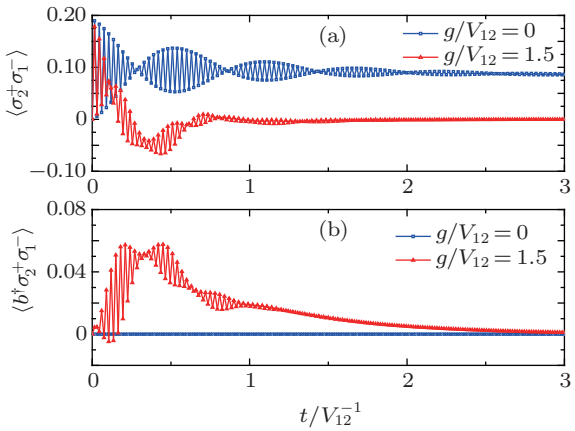


Fig. 4. (color online) Numerical results for dynamics of off-diagonal elements (a) $\langle\sigma_2^+\sigma_1^-\rangle$ and (b) $\langle b^\dagger\sigma_2^+\sigma_1^-\rangle$ with considering (red solid line with open up triangles) and without considering (blue solid line with open squares) the coupling between the donor and the vibrational mode. Other parameters used here are the same as those in Eq. (8).

Apart from the coherence between the donor and the acceptor $\langle\sigma_2^+\sigma_1^-\rangle$, we also calculate the coherence among the donor, the acceptor and the vibrational mode $\langle b^\dagger\sigma_2^+\sigma_1^-\rangle$. The result is shown in Fig. 4(b). Without coupling to the vibrational mode, there is no coherence among the donor, the acceptor and the vibrational mode during the energy transfer process. By contrast, the participation of the vibrational mode introduces coherence. The coherence reaches to its maximal value just at the time when the phonon-assisted energy transfer occurs. Shortly afterwards, the coherence decreases to zero with the completion of the energy transfer process. Now we say that the coupling to the vibrational mode introduces a resonant and coherent energy transfer process, among the donor, the acceptor and the vibrational mode, which dramatically improves the transfer efficiency and average transfer time.

In this section, we have numerically calculated the system's population dynamics and coherence dynamics to reveal that the coupling to vibrational mode introduces a coherent energy transfer process converting the original detuned energy transfer process to a resonant one. This coherent energy transfer process offers higher efficiency and shorter transfer time. We find that a larger coupling strength g gives more help in both efficiency and transfer time. The vibrational mode's initial state and dissipation only affect the EET slightly. The vibrational mode should be in resonant to the detuning to get the best transfer efficiency and the shortest transfer time.

4. Conclusion

The phonon-assisted process of energy transfer aiming at exploring the newly emerging frontier between biology and physics is an issue of central interest. In this paper, we have illustrated the important role of the high-energy intramolecular vibrational modes for efficient energy transport in photosynthetic systems, where excitonic states are highly localized because of the large energy gaps and relatively weak electronic interaction, like the PE545 antennae protein present in cryptophyte algae. We theoretically studied the effective interactions among the donor, the acceptor, and the high-energy vibrational mode by deriving an effective interaction Hamiltonian in the polaron frame. To quantify the impact of the high-energy vibrational mode upon the dynamics and efficiency of EET in our model, we also investigated the population dynamics and coherence dynamics of the system numerically. It is found that, the energy transfer efficiency and the transfer time depend heavily on the interaction strength of the donor and the high-energy vibrational mode, as well as the vibrational frequency. The numerical results also indicate that the initial state and dissipation rate of the vibrational mode hardly influence the dynamics of the dimer system.

In the above theoretical and numerical study, we only considered the intramolecular vibrational mode that couples to the donor. This model can not only capture the basic feature of detuned high-energy-phonon-assisted energy transfer, but also is pithy. In a more realistic situation, the acceptor molecule also couples to its own intramolecular vibrational mode, which offers an additional transition channel with the same mechanism of that studied above. In this case, energy can be transferred from the donor to the acceptor with the creation of a phonon in vibrational mode 1 (being coupled to the donor) or in vibrational mode 2 (being coupled to the acceptor) independently. With both of the channels working (according to the numerical results that are not shown here), the efficiency $\eta(t)$ increases a little more quickly and the steady value is slightly higher than that of the non-mode-2 case.

This study not only reveals the mechanism of the effective energy transfer in natural photosynthetic systems that have been optimized with the help of great evolution, but also offers an optimal design principle for artificial light-harvesting systems.

References

[1] Ishizaki A, Calhoun T R, Schlau-Cohen G S and Fleming G R 2010 *Phys. Chem. Chem. Phys.* **12** 7319

[2] Scholes G D, Fleming G R, Olaya-Castro A and van Grondelle R 2011 *Nat. Chem.* **3** 763

[3] Olaya-Castro A and Scholes G D 2011 *Int. Rev. Phys. Chem.* **30** 49

[4] Collini E 2013 *Chem. Soc. Rev.* **42** 4932

[5] Levi F, Mostarda S, Rao F and Mintert F 2015 *Rep. Prog. Phys.* **78** 082001

[6] Zhang Y P, Li H R, Fang A P, Chen H and Li F L 2013 *Chin. Phys. B* **22** 057104

[7] Tan Q S, Xu L and Kuang L M 2013 *Chin. Phys. B* **22** 010304

[8] Renger T, May V and Kühn O 2001 *Phys. Rep.* **343** 137

[9] Roden J, Schulz G, Eisfeld A and Briggs J 2009 *J. Chem. Phys.* **131** 044909

[10] Hossein-Nejad H, Olaya-Castro A and Scholes G D 2012 *J. Chem. Phys.* **136** 024112

[11] Renger T, Madjet M E, Knorr A and Müh F 2011 *J. Plant Physiol.* **168** 1497

[12] Feng L J, Zhang Y J, Zhang L and Xia Y J 2015 *Chin. Phys. B* **24** 110305

[13] Plenio M B and Huelga S F 2008 *New J. Phys.* **10** 113019

[14] Mohseni M, Rebentrost P, Lloyd S and Aspuru-Guzik A 2008 *J. Chem. Phys.* **129** 174106

[15] Shabani A, Mohseni M, Rabitz H and Lloyd S 2012 *Phys. Rev. E* **86** 011915

[16] Mohseni M, Shabani A, Lloyd S and Rabitz H 2014 *J. Chem. Phys.* **140** 035102

[17] Womick J M and Moran A M 2009 *J. Phys. Chem. B* **113** 15747

[18] West B A, Womick J M, McNeil L E, Tan K J and Moran A M 2011 *J. Phys. Chem. B* **115** 5157

[19] Rätsep M, Pieper J, Irrgang K D and Freiberg A 2008 *J. Phys. Chem. B* **112** 110

[20] Wendling M, Pullerits T, Przyjalgowski M A, Vulto S I E, Aartsma T J, van Grondelle R and van Amerongen H 2000 *J. Phys. Chem. B* **104** 5825

[21] Jankowiak R, Reppert M, Zazubovich V, Pieper J and Reinot T 2011 *Chem. Rev.* **111** 4546

[22] Eisenmayer T J, de Groot H J M, van de Wetering E, Neugebauer J and Buda F 2012 *J. Phys. Chem. Lett.* **3** 694

[23] Womick J M and Moran A M 2011 *J. Phys. Chem. B* **115** 1347

[24] Richards G H, Wilk K E, Curmi P M G, Quiney H M and Davis J A 2012 *J. Phys. Chem. Lett.* **3** 272

[25] Davydov A S 1971 *Theory of Molecular Excitons* (New York: Springer Science+Business Media) p. 169

[26] Yang M 2006 *J. Mol. Spectrosc.* **239** 108

[27] Doust A B, Marai C N J, Harrop S J, Wilk K E, Curmi P M G and Scholes G D 2004 *J. Mol. Biol.* **344** 135

[28] Kolli A, O'Reilly E J, Scholes G D and Olaya-Castro A 2012 *J. Chem. Phys.* **137** 174109

[29] Turner D B, Dinshaw R, Lee K-K, Belsley M S, Wilk K E, Curmi P M G and Scholes G D 2012 *Phys. Chem. Chem. Phys.* **14** 4857

[30] Ritschel G, Roden J, Strunz W T and Eisfeld A 2011 *New J. Phys.* **13** 113034

[31] Hay S and Scrutton N S 2012 *Nat. Chem.* **4** 161

[32] Wilk K E, Harrop S J, Jankova L, Edler D, Keenan G, Sharples F, Hiller R G and Curmi P M 1999 *Proc. Natl. Acad. Sci. USA* **96** 8901

[33] Jang S 2011 *J. Chem. Phys.* **135** 034105

[34] Kolli A, Nazir A and Olaya-Castro A 2011 *J. Chem. Phys.* **135** 154112

[35] Olaya-Castro A, Lee C F, Olsen F F and Johnson N F 2008 *Phys. Rev. B* **78** 085115

[36] Caruso F, Chin A W, Datta A, Huelga S F and Plenio M B 2009 *J. Chem. Phys.* **131** 105106

[37] Yang S, Xu D Z, Song Z and Sun C P 2010 *J. Chem. Phys.* **132** 234501

[38] Tan Q S and Kuang L M 2012 *Sci. China-Phys. Mech. Astron.* **55** 1541